Physics in Medicine & Biology

NOTE

Comparison of linear energy transfer scoring techniques in Monte Carlo simulations of proton beams

To cite this article: Dal A Granville and Gabriel O Sawakuchi 2015 *Phys. Med. Biol.* **60** N283

IOP Publishing | Institute of Physics and Engineering in Medicine Physics in Medicine & Biology

Phys. Med. Biol. **60** (2015) N283–N291 doi:10.1088/0031-9155/60/14/N283

Note

Comparison of linear energy transfer scoring techniques in Monte Carlo simulations of proton beams

Dal A Granville[1] **and Gabriel O Sawakuchi**[2,3]

[1] Carleton Laboratory for Radiotherapy Physics, Carleton University, Ottawa, Canada
[2] Department of Radiation Physics, The University of Texas MD Anderson Cancer Center, Houston, TX 77030, USA
[3] Graduate School of Biomedical Sciences, The University of Texas, Houston, TX 77030, USA

E-mail: dal.granville@carleton.ca and gsawakuchi@mdanderson.org

Received 2 April 2015, revised 14 May 2015
Accepted for publication 26 May 2015
Published 6 July 2015

Abstract

Monte Carlo (MC) simulations are commonly used to study linear energy transfer (LET) distributions in therapeutic proton beams. Various techniques have been used to score LET in MC simulations. The goal of this work was to compare LET distributions obtained using different LET scoring techniques and examine the sensitivity of these distributions to changes in commonly adjusted simulation parameters. We used three different techniques to score average proton LET in TOPAS, which is a MC platform based on the Geant4 simulation toolkit. We determined the sensitivity of each scoring technique to variations in the range production thresholds for secondary electrons and protons. We also compared the depth-LET distributions that we acquired using each technique in a simple monoenergetic proton beam and in a more clinically relevant modulated proton therapy beam. Distributions of both fluence-averaged LET (LET_Φ) and dose-averaged LET (LET_D) were studied. We found that LET_D values varied more between different scoring techniques than the LET_Φ values did, and different LET scoring techniques showed different sensitivities to changes in simulation parameters.

Keywords: proton therapy, linear energy transfer, Monte Carlo

(Some figures may appear in colour only in the online journal)

1. Introduction

The relative biological effectiveness of proton beams varies with linear energy transfer (LET). Thus, researchers have investigated the use of LET in the optimization of proton therapy

treatment plans (Krämer and Scholz 2000, Wilkens and Oelfke 2006, Grassberger *et al* 2011, Giantsoudi *et al* 2013). Because LET is not easily measurable, Monte Carlo (MC) simulations are often used to determine LET distributions. Researchers have used a variety of MC platforms to determine LET distributions, including Geant4 (Cirrone *et al* 2011, Grassberger *et al* 2011, Grassberger and Paganetti 2011, Chen and Ahmad 2012, Romano *et al* 2014, Cortés-Giraldo and Carabe 2015), MCNPX (Sawakuchi *et al* 2010, Wang *et al* 2012, Johansson *et al* 2013, Perles *et al* 2013, Robertson *et al* 2013), FLUKA (Kantemiris *et al* 2011) and TOPAS, which is based on the Geant4 toolkit (Carabe *et al* 2012, Perl *et al* 2012, Giantsoudi *et al* 2013, Zeng *et al* 2013, Granville *et al* 2014, Sethi *et al* 2014).

Average LET values are often calculated in one of two ways: using a fluence-weighted average (LET_Φ) or a dose-weighted average (LET_D). Generally, LET_D is thought to better correlate with biological damage and is more commonly used. To the best of our knowledge, however, the superiority of LET_D over LET_Φ has not been rigorously demonstrated in therapeutic proton beams. Both LET_Φ and LET_D have been scored using a variety of techniques and simulation parameters. Several investigators have used a technique in which LET is scored on a step-by-step basis using the ratio of energy deposition to step-length (Grassberger and Paganetti 2011, Grassberger *et al* 2011, Chen and Ahmad 2012). A second step-by-step approach involves using the pre-step proton kinetic energy to calculate the theoretical LET (Granville and Sawakuchi 2014, Cortés-Giraldo and Carabe 2015). A third approach is to score the proton energy spectrum inside a voxel and convert to an LET spectrum after the simulation, from which average LET values can be calculated (Sawakuchi *et al* 2010, Cirrone *et al* 2011, Perles *et al* 2013, Granville *et al* 2014). A fourth approach uses the relationship between absorbed dose, fluence, and LET to calculate LET_Φ by dividing the absorbed dose within a voxel by the fluence within the same voxel (Wang *et al* 2012, Robertson *et al* 2013).

Cortés-Giraldo and Carabe recently compared primary proton LET_D distributions obtained using the ratio of energy deposition to step-length and the computation of LET from pre-step kinetic energy (Cortés-Giraldo and Carabe 2015). They found that computing LET using pre-step kinetic energy resulted in LET_D distributions that were insensitive to variations in simulation parameters including voxel thickness and secondary electron production thresholds, and better agreed with microdosimetric simulations of dose-mean lineal energy. Grassberger and Paganetti (Grassberger and Paganetti 2011) have demonstrated the sizable effects of including secondary protons in the calculation of LET_D.

The goals of this study were to investigate the sensitivity of different LET scoring techniques to variations in simulation parameters, namely the secondary electron and proton production thresholds, and to compare LET distributions obtained using different scoring techniques. We emphasize that our aim was not to determine the most 'accurate' method of scoring LET, because we do not have a gold standard measurement to compare with. We build upon Cortés-Giraldo and Carabe's results by including secondary protons in the LET scoring, investigating LET_Φ distributions, studying an additional LET scoring technique (energy spectrum technique), and investigating the dependence of LET on Geant4 secondary proton production thresholds.

2. Methods

2.1. Simulation details

We used TOPAS version 1.0-b12, which is based on the Geant4 v4.09.06-p02 simulation toolkit. Two different beams were simulated: 1) a 150 MeV monoenergetic proton beam; and 2) a

modulated 200 MeV beam with a 10 cm spread-out Bragg peak (SOBP). The modulated beam was produced using a validated model of a passive scattering proton therapy nozzle from The University of Texas MD Anderson Cancer Center Proton Therapy Center in Houston, TX (Chequers *et al* 2012). All beams were incident on a cylindrical water tank that was 32 cm long with a 10 cm radius. The tank was divided into 1 mm voxels depth-wise.

We used Geant4 range production thresholds between 0.01 mm and 100 mm for electrons and between 0.001 and 1 mm for protons. All protons (primary and secondary) were included in the LET scoring. Other secondary particles were transported (with the TOPAS default production threshold of 0.05 mm) but were not included in the LET scoring. The maximum step size parameter (100 mm), finalRange parameter (0.1 mm for electrons, 0.05 mm for protons) and all other simulation parameters were set to the default values. We used the TOPAS default physics list, which has been validated for proton therapy simulations. Statistical uncertainties in LET_Φ and LET_D and were better than 0.05% and 0.5%, respectively, for all conditions in which the LET scoring techniques were found to provide reliable results.

2.2. LET scoring techniques

2.2.1. Technique 1: energy deposition. With technique 1, LET was scored step-by-step by summing the energy deposited locally by a proton with the kinetic energies of secondary electrons generated during each step. The resulting energy was divided by the step-length to determine LET for each step (LET_i). The proton local energy loss was determined with the Geant4 method GetTotalEnergyDeposit().

By using appropriate weighting factors, we calculated both LET_Φ and LET_D with this technique. The sum of step lengths in a voxel is directly proportional to the fluence within that voxel (Chilton 1978, 1979, Papiez and Battista 1994). To obtain LET_Φ, we multiplied LET of each step (i) by the length of that step ($\mathrm{d}x_i$). After simulation, the sum of these dx-weighted LET values was divided by the sum of $\mathrm{d}x_i$ for all steps.

$$\mathrm{LET}_\Phi = \frac{\sum_i^N \mathrm{d}x_i \times \mathrm{LET}_i}{\sum_i^N \mathrm{d}x_i} \tag{1}$$

Note that when weighting by fluence (or, equivalently, $\mathrm{d}x_i$), this technique is equivalent to scoring absorbed dose (or energy deposited) within a volume and dividing that by the fluence within the volume, because $\mathrm{d}x_i \times \mathrm{LET}_i = \mathrm{d}x_i \times E_\mathrm{dep}/\mathrm{d}x_i = E_\mathrm{dep}$.

To obtain LET_D, we multiplied LET for each step i by $E_{\mathrm{dep,i}}$, the energy deposited during that step. The sum of these E_dep-weighted LET values was then divided by the total energy deposited for each voxel, after simulation.

$$\mathrm{LET}_\mathrm{D} = \frac{\sum_i^N E_{\mathrm{dep},i} \times \mathrm{LET}_i}{\sum_i^N E_{\mathrm{dep},i}} \tag{2}$$

Note that the LET_D scoring technique was built in to TOPAS, whereas we created the LET_Φ scorer with a user-written extension.

2.2.2. Technique 2: dE/dx computation. With this technique, LET_i was determined on the basis of proton kinetic energy at the beginning of each proton step. This was accomplished using the Geant4 method ComputeElectronicDEDX(), which computes the unrestricted electronic stopping power (numerically equivalent to the unrestricted LET). This technique was used to score both LET_Φ and LET_D by weighting the LET values in the same manner as described for technique 1. Note that we implemented this scorer in TOPAS with a user-written extension.

2.2.3. Technique 3: energy spectrum. For this technique, we scored the proton fluence as a function of kinetic energy. After simulation, the resulting energy spectrum was converted to an LET spectrum using a lookup table (Berger *et al* 1998). The LET spectrum was then used to calculate both LET_Φ and LET_D according to the following formulae:

$$LET_\Phi = \frac{\sum_j^N \Phi_j \times LET_j}{\sum_j^N \Phi_j} \tag{3}$$

and

$$LET_D = \frac{\sum_j^N \Phi_j \times LET_j \times LET_j}{\sum_j^N \Phi_j \times LET_j}, \tag{4}$$

where N is the number of bins in the LET spectrum, j is the jth LET bin, Φ_j is the proton fluence in the jth bin, and LET_j is the value of the jth bin. We implemented this method with a user-written TOPAS extension.

This technique is expected to show some sensitivity to the width of energy bins. We tested two bin widths: 0.1 MeV and 0.01 MeV. We found a maximum discrepancy of 0.12% between the resulting LET_D values for depths in water up to the 10% distal falloff in the 150 MeV monoenergetic beam. Discrepancies in the 200 MeV 10 cm SOBP beam were a maximum of 0.62%. LET_Φ values were even less sensitive to changes in bin width. All results shown for technique 3 were acquired using a bin width of 0.1 MeV.

3. Results

3.1. Dependence on secondary electron production threshold

Figure 1 shows depth-LET distributions obtained using technique 1 in the 150 MeV monoenergetic proton beam and the 200 MeV modulated beam. The depth-LET_D distributions obtained using technique 1 were heavily dependent on the secondary electron production threshold. As the threshold was lowered, LET_D values increased. In the monoenergetic beam (figure 1(a)), for thresholds of 0.1 mm and lower, the depth-LET_D curves were not smooth, exhibiting a number of spikes. For thresholds greater than 1 mm, however, the curves were smooth and consistent with one another. Results for the 200 MeV modulated beam were qualitatively similar. For clarity, only the largest and smallest secondary electron production thresholds are shown (0.01 mm and 100 mm) for the modulated beam (figure 1(b)).

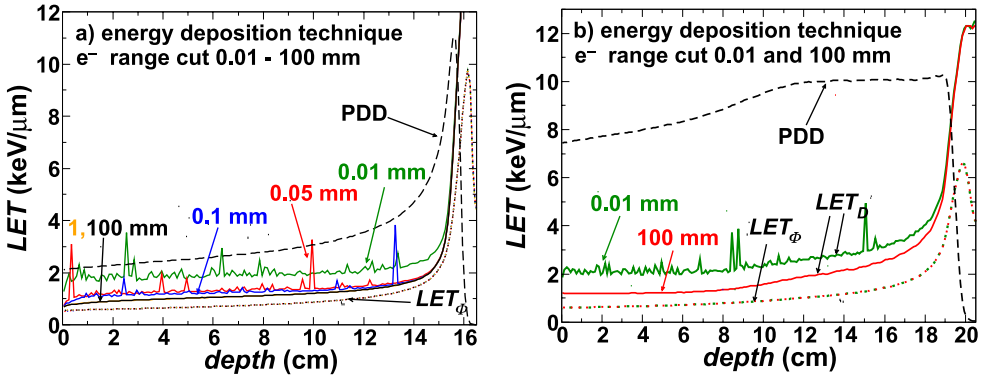

Figure 1. LET_D (solid lines) and LET_Φ (dotted lines) versus depth in water for (a) a 150 MeV monoenergetic proton beam and (b) a 200 MeV beam with a 10 cm SOBP. Results were obtained using technique 1, the energy deposition technique. Individual secondary electron production thresholds are labeled where the results are distinguishable from one another. PDD indicates percentage depth dose and is included as a guide to the eye.

Depth-LET_D curves obtained with techniques 2 and 3 showed only a small dependence on the secondary electron production threshold. At depths shallower than the 10% distal falloff in dose, reduction of the threshold from 100 mm to 0.01 mm resulted in an average LET_D increase of 0.83% and 1.00% for technique 2, and 0.99% and 1.25% for technique 3 in the monoenergetic and modulated beams, respectively. The depth-LET_Φ distributions for all scoring techniques showed even smaller dependence on the secondary electron production threshold. These results were obtained using a secondary proton production threshold of 0.05 mm (TOPAS default).

3.2. Dependence on secondary proton production threshold

Depth-LET_D and depth-LET_Φ distributions obtained using techniques 1, 2, and 3 in the 150 MeV monoenergetic beam and 200 MeV modulated beam showed no strong dependence on the secondary proton production threshold. Reducing the secondary proton production threshold from the highest value (1 mm) to the lowest value (0.001 mm) investigated resulted in average LET_D increases of just 0.069%, 0.13% and 0.21% using techniques 1, 2 and 3 respectively at depths shallower than the 10% distal falloff in the 150 MeV monoenergetic beam, and even smaller increases in the 200 MeV modulated beam. LET_Φ showed even less dependence on secondary proton production thresholds. Note that the secondary electron production threshold was set to 100 mm for these simulations, to eliminate the problems associated with scoring LET_D with technique 1.

3.3. Scoring technique comparison

Figure 2 shows the depth-LET distributions obtained with each scoring technique in the 150 MeV monoenergetic proton beam and 200 MeV modulated beam. In both beams, LET_D values obtained using technique 1 were consistently higher than those obtained using technique 2, and those obtained using technique 3 were lower still. LET_Φ values, however, showed little difference between the three techniques. Differences of up to about 17.5% occurred in LET_D values in the plateau region of the 150 MeV monoenergetic beam

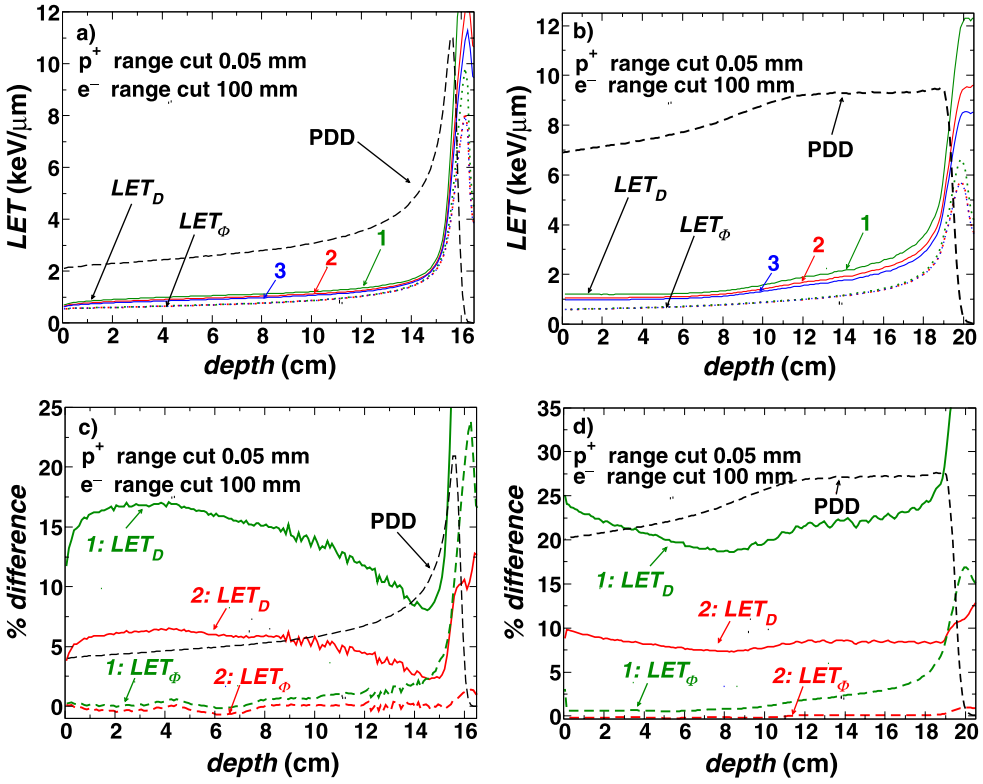

Figure 2. (a) Comparison among LET_D (solid lines) and LET_Φ (dotted lines) distributions in a 150 MeV monoenergetic proton beam obtained using technique 1 (green), 2 (red), or 3 (blue). (b) Comparison among LET_D and LET_Φ distributions in a modulated 200 MeV proton beam with a 10 cm SOBP obtained using technique 1, 2 or 3. (c) Percentage differences among LET_D and LET_Φ values obtained using different techniques at each depth in water in the 150 MeV monoenergetic beam. Differences between techniques 1 and 2 with respect to technique 3 are shown. (d) Percentage differences among LET_D and LET_Φ values obtained using different techniques at each depth in water in the 200 MeV modulated beam.

between techniques 1 and 3, and differences of up to about 7% occurred between techniques 2 and 3. Even larger differences occurred near the Bragg peak. Differences in LET_Φ values were much smaller, remaining below 5% until depths beyond the Bragg peak in the comparison between techniques 1 and 3. Differences between LET_Φ values using techniques 2 and 3 were smaller than about 2%. Discrepancies among values obtained using the 3 different scoring techniques were generally larger in the modulated beam than in the monoenergetic beam. In the modulated beam, discrepancies among LET_D values were highest (about 25%) in the entrance region and near the end of the SOBP. Discrepancies among LET_Φ values were smaller than 5% until the end of the SOBP, where they rose to about 15%. These data were generated with a secondary electron production threshold of 100 mm, as technique 1 was shown previously to be unreliable for low secondary electron production threshold values (figure 1). The secondary proton production threshold was 0.05 mm (TOPAS default).

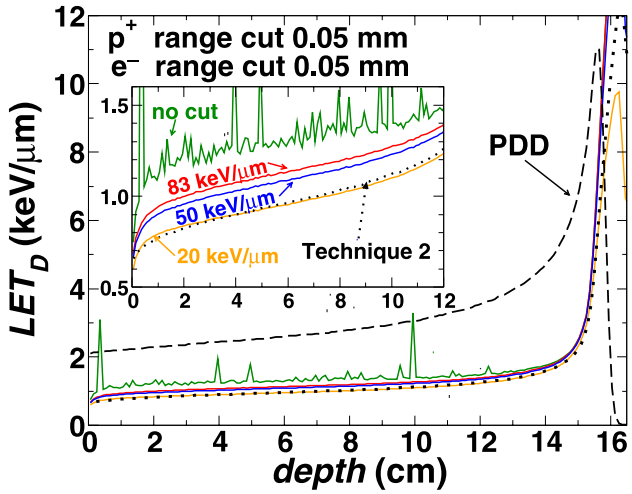

Figure 3. Comparison between depth-LET_D curves obtained using technique 1 and three different high-LET cutoff values of 83 (corresponding approximately to the maximum theoretical proton LET), 50 and 20 keV/μm. For comparison, the depth-LET_D curve obtained using technique 2 for the same simulation conditions is shown. Results are shown using the default TOPAS secondary electron and proton production thresholds of 0.05 mm. The inset represents the same plotted data in magnified y-axis scale.

4. Discussion and conclusions

4.1. Dependence on secondary electron production threshold

Ideally, the production threshold for secondary electrons should have no major effects on the resulting proton LET distributions in MC simulations. Cortés-Giraldo and Carabe demonstrated that primary proton depth-LET_D curves calculated using technique 1 showed strong dependence on the secondary electron production threshold and provided spurious results for thresholds of 0.2 mm and below, while results obtained using technique 2 were smooth and consistent (Cortés-Giraldo and Carabe 2015). Our results, which scored total proton LET_D (including secondaries), qualitatively agree with those found by Cortés-Giraldo and Carabe for techniques 1 and 2. In addition, our results demonstrate that the problems associated with technique 1 can be eliminated by using a high secondary electron production threshold (1 mm or greater). Further, our results demonstrate that technique 3, similarly to technique 2, shows minimal dependence on secondary electron production thresholds.

The physical basis of technique 1's dependence on secondary electron production threshold has been explained in the literature (Cortés-Giraldo and Carabe 2015). In short, high LET values occur when a secondary electron is produced during a proton step that has its length greatly shortened due to a voxel boundary. Increasing the secondary electron production threshold eliminates this effect by drastically reducing the number of secondary electrons explicitly produced. Generally, for simulations relevant to proton therapy, increasing the secondary electron production threshold has only small effects on the resulting dose distributions and greatly reduces computation time. Thus, increasing the secondary electron production threshold can be a useful approach to the problems associated with technique 1.

Cortés-Giraldo and Carabe proposed an approach to the spurious LET_D results obtained with technique 1 by considering the entire energy deposition and step length per voxel for

each proton, rather than a step-by-step calculation. This resulted in smoother LET_D distributions, but showed a dependence on voxel thickness (Cortés-Giraldo and Carabe 2015). We considered a second approach, which involved a high-LET cutoff value to discriminate against large, unphysical LET values during a given step. The downside of this approach is that the cutoff value is somewhat arbitrary, and we found that the results were highly dependent on the cutoff value chosen (figure 3).

All LET_Φ scoring techniques showed only a small dependence on secondary electron production thresholds. The problems associated with technique 1 are not present when scoring LET_Φ because the step length value is cancelled out in the fluence weighting.

4.2. Dependence on secondary proton production threshold

Our results showed only a small dependence of LET on secondary proton production thresholds in the range of 0.001 to 1 mm. Contrary to our results, decreasing secondary proton production thresholds might be expected to cause a large increase average proton LET, because this would increase the number of low-energy (high-LET) protons present in the simulation. It is important to note that the secondary proton production threshold in Geant4 (which TOPAS is based on) is not a universal threshold; it applies only to secondary protons resulting from *elastic* processes. Thus, MC codes that institute a universal cutoff for secondary proton production may exhibit greater dependence on the secondary proton production threshold. We have not shown results for secondary proton production thresholds larger than the voxel thickness (1 mm). Very high thresholds do result in lower LET values, however such high thresholds are impractical when we are interested in spatial accuracy on the order of 1 mm.

4.3. Scoring technique comparison

It is evident from figure 2 that the choice of scoring technique does affect the resulting LET values. Several recommendations can be made based on our data. Technique 1 provided unreliable values of LET_D when low secondary electron production thresholds were used. Technique 3 provided self-consistent results and was insensitive to changes in simulation parameters. However, this technique required on-the-fly binning and storage of more data during simulation than the others. In addition, the energy binning could lead to inaccuracies, particularly at low energies where the LET changes rapidly with energy. Based on our data, it is reasonable to conclude that the dE/dx computation technique (technique 2) is the most advantageous for scoring LET_D distributions in proton therapy beams. In addition, Cortés-Giraldo and Carabe demonstrated that technique 2 best agrees with microdosimetric simulations of dose-mean lineal energy (Cortés-Giraldo and Carabe 2015). For simulations of LET_Φ, however, there is no clear advantage to choosing either technique 1 or 2.

Acknowledgments

The authors would like to thank the TOPAS Collaboration for providing access to the TOPAS code, and for helpful discussions. DAG was supported by the Natural Sciences and Engineering Research Council of Canada CGS-D while performing this research.

References

Berger M J, Coursey J S, Zucker M A and Chang J 1998 *Stopping-Power and Range Tables for Electrons, Protons, and Helium Ions* (Gaithersburg, MD: NIST Physical Measurement Laboratory)

Carabe A, Moteabbed M, Depauw N, Schuemann J and Paganetti H 2012 Range uncertainty in proton therapy due to variable biological effectiveness *Phys. Med. Biol.* **57** 1159–72
Chen Y and Ahmad S 2012 Empirical model estimation of relative biological effectiveness for proton beam therapy *Radiat. Prot. Dosim.* **149** 116–23
Chequers M H, Granville D, Suzuki K and Sawakuchi G O 2012 A time dependent model of a passive scattering proton therapy nozzle using TOPAS *Med. Phys.* **39** 3718
Chilton A 1978 A note on the fluence concept *Health Phys.* **34** 715–6
Chilton A 1979 Further comments on an alternative definition of fluence *Health Phys.* **36** 637–8
Cirrone G A P *et al* 2011 Hadrontherapy : a Geant4-based tool for proton/ion-therapy studies *Prog. Nucl. Sci. Technol.* **2** 207–12
Cortés-Giraldo M A and Carabe A 2015 A critical study of different Monte Carlo scoring methods of dose average linear-energy-transfer maps calculated in voxelized geometries irradiated with clinical proton beams *Phys. Med. Biol.* **60** 2645–69
Giantsoudi D, Grassberger C, Craft D, Niemierko A, Trofimov A and Paganetti H 2013 Linear energy transfer-guided optimization in intensity modulated proton therapy: feasibility study and clinical potential *Int. J. Radiat. Oncol. Biol. Phys.* **87** 216–22
Granville D A, Sahoo N and Sawakuchi G O 2014 Calibration of the Al_2O_3:C optically stimulated luminescence (OSL) signal for linear energy transfer (LET) measurements in therapeutic proton beams *Phys. Med. Biol.* **59** 4295–310
Granville D A and Sawakuchi G O 2014 Comparison of different Monte Carlo methods of scoring linear energy transfer in modulated proton therapy beams *Med. Phys.* **41** 16
Grassberger C and Paganetti H 2011 Elevated LET components in clinical proton beams *Phys. Med. Biol.* **56** 6677–91
Grassberger C, Trofimov A, Lomax A and Paganetti H 2011 Variations in linear energy transfer within clinical proton therapy fields and the potential for biological treatment planning *Int. J. Radiat. Oncol. Biol. Phys.* **80** 1559–66
Johansson E, Andersson J, Johansson L and Tölli H 2013 Liquid ionization chamber initial recombination dependence on LET for electrons and photons *Phys. Med. Biol.* **58** 4225–36
Kantemiris I, Karaiskos P, Papagiannis P and Angelopolous A 2011 Dose and dose averaged LET comparison of 1H, 4He, 6Li, 8Be, 10B, 12C, 14N, and 16O ion beams forming a spread-out Bragg peak *Med. Phys.* **38** 6585–91
Krämer M and Scholz M 2000 Treatment planning for heavy-ion radiotherapy: calculation and optimization of biologically effective dose *Phys. Med. Biol.* **45** 3319–30
Papiez L and Battista J J 1994 Radiance and particle fluence *Phys. Med. Biol.* **39** 1053–62
Perl J, Shin J, Schumann J, Faddegon B and Paganetti H 2012 TOPAS: an innovative proton Monte Carlo platform for research *Med. Phys.* **39** 6818–37
Perles L A, Mirkovic D, Anand A, Titt U and Mohan R 2013 LET dependence of the response of EBT2 films in proton dosimetry modeled as a bimolecular chemical reaction *Phys. Med. Biol.* **58** 8477–91
Robertson D, Mirkovic D, Sahoo N and Beddar S 2013 Quenching correction for volumetric scintillation dosimetry of proton beams *Phys. Med. Biol.* **58** 261–73
Romano F, Cirrone G A P, Cuttone G, Di Rosa F, Mazzaglia S E, Petrovic I, Ristic Fira A and Varisano A 2014 A Monte Carlo study for the calculation of the average linear energy transfer (LET) distributions for a clinical proton beam line and a radiobiological carbon ion beam line *Phys. Med. Biol.* **59** 2863–82
Sawakuchi G O, Sahoo N, Gasparian P B R, Rodriguez M G, Archambault L, Titt U and Yukihara E G 2010 Determination of average LET of therapeutic proton beams using Al_2O_3:C optically stimulated luminescence (OSL) detectors *Phys. Med. Biol.* **55** 4963–76
Sethi R V *et al* 2014 Patterns of failure after proton therapy in medulloblastoma; linear energy transfer distributions and relative biological effectiveness associations for relapses *Int. J. Radiat. Oncol. Biol. Phys.* **88** 655–63
Wang L L W, Perles L A, Archambault L, Sahoo N, Mirkovic D and Beddar S 2012 Determination of the quenching correction factors for plastic scintillation detectors in therapeutic high-energy proton beams *Phys. Med. Biol.* **57** 7767–81
Wilkens J J and Oelfke U 2006 Fast multifield optimization of the biological effect in ion therapy *Phys. Med. Biol.* **51** 3127–40
Zeng C, Giantsoudi D, Grassberger C, Goldberg S, Niemierko A, Paganetti H, Efstathiou J A and Trofimov A 2013 Maximizing the biological effect of proton dose delivered with scanned beams via inhomogeneous daily dose distributions *Med. Phys.* **40** 051708–1–9